IRANIAN SOCIETY of CRYSTALLOGRAPHY and MINERALOGY

Vol.19, No. 1, Spring 1390/2011

Pages 1 to 18

IRANIAN JOURNAL of CRYSTALLOGRAPHY and MINERALOGY

U-Pb zircon geochronology and Sr-Nd isotopic characteristic of Late Neoproterozoic Bornaward granitoids (Taknar zone exotic block), Iran

M.H. Karimpour[1*], G. Lang Farmer[2], C.R. Stern[2], E. Salati[1]

1. Research Center for Ore Deposit of Eastern Iran, Ferdowsi University of Mashhad, Iran
Dept. of Geological Sciences, University of Colorado, CB-399, Boulder, CO, USA

(Received: 10/5/2010, in revised form: 14/7/2010)

Abstract: The study area (Bornaward granite) is located in northeast of Iran (Khorasan Razavi province), about 280 km southwest of Mashhad city. Taknar zone is an exotic block, bordered by two major faults, Great Kavir fault (Drouneh) to the south and Rivash fault in the north. A complex of granite, granodiorite, monzonite and diorite crop out at the center of Taknar zone. They are named as "Bornaward granite". Published data using Rb–Sr whole-rock and biotite isotopic methods on granitoid rocks (Bornaward granite) gave ages of 154 to 111 Ma. The results of U-Pb zircon dating of granodiorite is 552.69 ± 10.89 Ma and granite is 538.22 – 1.82, + 4.28 Ma (Late Neoproterozoic time). Both granite and granodiorite are classified as belonging to the ilmenite-series of reduced S-type granitoids. Chemically, they are per-aluminous, high-K calc-alkaline with relatively enriched in LILE, Rb, K and depleted in Sr, Ba, Nb, Ti, Ta, Y and Yb. Chondrite-normalized Rare Earth Element (REE) plots indicate minor enrichments of light REE in composition with heavy REE, with $(La/Yb)_N$ between 3.5-5.6 and high total REE (193-252) with strong negative anomaly of Eu. They have a initial $^{87}Sr/^{86}Sr$ and $^{143}Nd/^{144}Nd$ ranging from 0.713566 to 0.716888 and 0.511791 to 0.511842, respectively, when recalculated to an age of 553 and 538 Ma, consistent with the new radiometric results. Initial εNd isotope values for granite and granodiorite range from -2.62 to -2.01. Granite and granodiorite of Bornaward yields a T_{DM} age of 1.4-1.41 Ga. This indicates that the granites and granodiorite being derived from partial melting of distinct basement source regions with very high initial $^{87}Sr/^{86}Sr$.

Keywords: *Taknar; Bornaward; Rb-Nd; U-Pb-zircon; late Neoproterozoic*.

Introduction

The study area (Taknar mine area) is located in northeast of Iran (Khorasan Razavi province), about 280 km southwest of Mashhad city and 28 km northwest of Bardaskan (Fig. 1). Taknar zone consists of Precambrian, Paleozoic, Mesozoic and Tertiary rocks [1-3]. Taknar zone is an exotic block bordered by two major faults, Great Kavir fault (Drouneh) to the south and Rivash fault in the north (Fig. 1).

Taknar Formation covers a large area within the Taknar zone. Based on the previous studies, age of Taknar Formation is Precambrian [1]. However, recent Palynological studies show that the age of Taknar Formation is Ordovician [4].

We found that the initial $^{87}Sr/^{86}Sr$ and age published by Soltani [5] is incorrect. Based on paleontological studies, the age of Taknar Formation is Ordovician [4]. Since the age of granitoid which are intruded Taknar Formation are Precambrian (present study), therefore this age is also incorrect. We present the results of new radiogenic isotope analyses and more accurate U-Pb in zircon age dating and discuss the paleotectonic and petrogenetic implications of these new data for Bornaward Neoproterozoic granitoid.

* Corresponding author, Telefax: (0511) 8797275, Email: mhkarimpour@yahoo.com

Geology

Taknar Formation is divided into lower, middle and upper members [1]. The lower member crops out in the central part of Taknar with thickness of 1500m. The lower member consists of meta-tuff and meta rhyolite. The middle member is exposed along the northern and southern margins of the Taknar zone [1]. The thickness of middle member varies between 150 to 350m [1]. It consists of alternation of meta–carbonate and quartzite with minor meta-rhyolite. The Upper member consists of fine to coarse-grained meta –graywakes (slate to phylite). Between Dahan Qaleh and Drouneh, the upper Taknar Formation is followed by Infracambrian and Early paleozoic dolomite and quartzite [1].

A complex of intrusive rocks crop out at the eithen of Taknar zone (Fig. 2). They are named as "Bornaward granite" [3, 6, 7]. The intrusive rocks are composed of granite, granodiorite, monzonite and diorite [8]. Granite and granodiorite are dominant. Based on field observation, diorite is older than granite and granodiorite [8]. Several episodes of magmatism were recognized at Taknar (Bornaward granitoid) [8]. Soltani [5] did some Rb-Sr analyses and calculated the age of intrusive rocks between 154 to 111 Ma. This age is not correct (See below). Petrography of intrusive and metamorphic rocks was studied by Homam [9] and Sepahigrou [10]. Zirjanizadeh [11] worked on petrography, major oxides and trace elements of intrusive rocks. Detail field work, petrography, Petrogenesis, radio isotopes and U-Pb zircon age are carried by the author.

Taknar mine is a magnetite-rich polymetal (Cu, Zn, Au, Ag, and Pb) massive sulfide deposit [12]. Mineralization shows good layering, therefore, it is a syngenetic deposit type and was formed at certain horizon within the upper member of Taknar Formation [12, 13]. Malekzadeh and Ghoorchi worked on the geology, alteration and mineralization of Taknar deposit [12, 13]. Based on local name, from north to south, deposits are named as Tak-II, Tak-I, Tak-IV and Tak-III.

Several episodes of metamorphism have affected the Taknar Formation and the intrusive rocks.

1- In areas where the polymetal massive sulfides are formed, the rocks are altered due to hydrothermal fluid; different types of alteration zones such as chlorite, sericite-chlorite, chlorite-carbonate and silicification were formed [12].

2- Contact metamorphism was developed at the contact of intrusive rocks with Taknar Formation.

3- Taknar Formation and most of the intrusive rocks were subjected to low-grade regional metamorphism. Slate and sericite-chlorite schist were formed within some parts of the Taknar Formation (areas with tuff, shale and graywacke). Regional metamorphism may have occurred at different episodes. 1- Precambrian during and after the granitoids intrusion; 2- Late Paleozoic; and 3- Middle Jurassic.

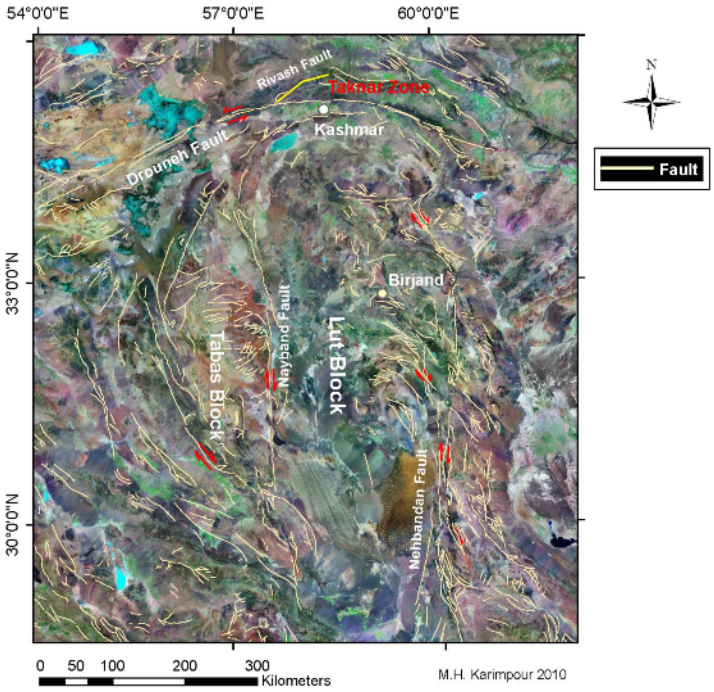

Figure 1. Taknar zone is shown on Landsat image.

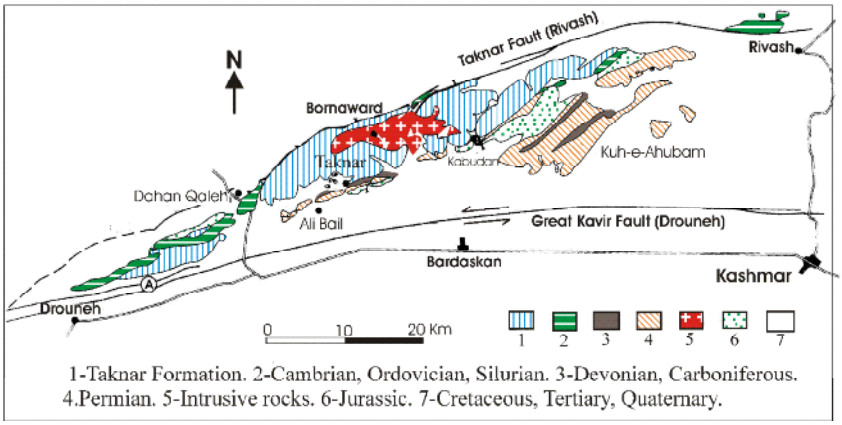

Figure 2. Geological map of the Taknar zone [1].

Taknar zone is an exotic block and it is located between two major faults, therefore since Precambrian, major displacement took place. Both right and left-lateral strike-slip faults are observed in the study area (Fig 2, 3). At least three generations of strike-slip faults are observed trending: 1- NE-SW, 2- NW-SE and 3- N-S.

Analytical Techniques

Bulk-rock chemistry

Major elements were analyzed by wavelength-dispersion X-ray fluorescence spectrometry (XRF) using fused discs. Pressed powder pellets were used for Zr, Nb, Sn, Sr, Ba, Sc, Y and Ga measurements by XRF (The XRF spectrometer used in this study was a Philips PW 1410) at Ferdowsi University of Mashhad, Iran. REE and trace elements composition of rocks was determined by ICP-MS in Canada (Acme Lab. Canada).

U/Pb dating

Two rock samples, which were both analyzed for Sr and Nd isotopes, were chosen for zircon U-Pb age dating. Zircons were isolated using standard mineral separation techniques. From each rock about 70 zircon grains were separated. Zircons were mounted along with a zircon standard and a couple of chips of NBS 610 Trace Element Glass in epoxy and polished down to 20 µm. Zircon age dating was done at the Arizona LaserChron Center with the method of Gehrels, and Valencia, (2006). Cathode-luminescence (CL) images are acquired for samples to be analyzed because they provide a powerful tool for placing laser pits in homogeneous portions of crystals, and also can help determine the origin (e.g., igneous, metamorphic, hydrothermal) of zircon grains. Laser ablation takes place with a beam diameter of either 35 or 25 microns for most applications, or with a beam diameter of 15 or 10 microns if finer spatial resolution is needed. With a 35 or 25 micron beam, the laser is set at a repetition rate of 8 Hz and energy of 100 mJ, which excavates at a rate of ~1 micron per second. This generates a signal of ~100,000 cps per ppm for U in zircon. For smaller beam sizes, the ablation rate is reduced to ~0.5 micron/second by reducing the laser energy (60 mJ) and repetition rate (4 Hz). In both cases the ablated material is removed from the ablation chamber in He carrier gas. The carrier gas (and sample) are then mixed with Ar gas before entering the plasma of the Inductively Coupled Plasma Mass Spectrometer (ICPMS). Isotopic analysis is performed with a Multicollector Inductively Coupled Plasma Mass Spectrometer (GVI Isoprobe) that is equipped with an S-option interface. The instrument is equipped with a collision cell that is operated with a flow rate of 0.2 ml/min of argon to create a uniform energy distribution, and the accelerating voltage is ~6 kV. Collectors include nine Faraday detectors and four low-side channeltron multipliers, all of which are moveable, as well as an axial Daly photomultiplier.

Nd–Sr isotopes

Sr and Nd isotopic analyses were performed on a 6-collector Finnigan MAT 261 Thermal Ionization Mass Spectrometer at the University of Colorado, Boulder (USA). $^{87}Sr/^{86}Sr$ ratios were analyzed using four-collector static mode measurements. Thirty measurements of SRM-987 during study period yielded mean $^{87}Sr/^{86}Sr=0.71032 \pm 2$ (error is the 2 sigma mean). Measured $^{87}Sr/^{86}Sr$ were corrected to SRM-987= 0.71028. Error in the 2 sigmas of mean refer to last two digits of the $^{87}Sr/^{86}Sr$ ratio. Measured $^{143}Nd/^{144}Nd$ normalized to $^{146}Nd/^{144}Nd=0.7219$. Analyses were dynamic mode, three-collector measurements. Thirty-three

measurements of the La Jolla Nd standard during the study period yielded a mean $^{143}Nd/^{144}Nd=0.511838 \pm 8$ (error is the 2 sigma mean).

Petrography

The granitic rocks of the Bornaward cut through the metamorphic rocks of the Taknar Formation. Based on field investigations and microscopic studies, several intrusive rocks are recognized in the study area (Figs. 3, 4). They are mainly granite, granodiorite and minor diorite-gabbro. Since the Taknar zone is an exotic block and it is surrounded by two major faults (Drouneh and Taknar), several system of faulting are recognized within the Taknar zone. The majority of the faults are strick-slip. One of the right lateral strick-slip fault cut the granitic rocks and the massive sulfide ore body with about 500 meter displacement (Figs. 3, 4). Both regional metamorphism and faulting caused some changes in fabric of the granitic rocks. In some locations, along the fault gneissic texture was formed.

Granite & biotite-granite: These rocks crop out in both Tak-I and Tak II (Figs. 3, 4). It has graphic to granular textures. In Some locations granite is strongly deformed with a NEE– trending foliation. The granite contains 45%–50% quartz, 30%–35% K- feldspar, 5% plagioclase, and 1-5% green biotite. Accessory minerals are zircon, and ilmenite.

Granodiorite: This unit also crops out in both Tak-I and Tak II, in Tak-I it cuts massive sulfide ore body and Taknar Formation (Figs. 3, 4). The texture is porphyry with some graphic intergrowth. Granodiorite contains 10% quartz (phenocrysts), 3-7% K- feldspar, 5-8% plagioclase, and 0.5 % biotite. Accessory minerals are zircon, and ilmenite. Quartz as veinlets formed near the contact of granodiorite with country rocks.

Gabbro-diorite: It crops out near massive sulfide ore bodies both in Tak-I and Tak II (Figs. 3, 4). Since it doesn't have zircon, therefore, we could not get the age of this rock based on U-Pb in zircon. Based on field observation and chemical composition (low SiO_2, met-aluminous, volcanic arc setting) it seems that the gabbro-diorite is older than granite and granodiorite. Stockwork mineralization (quartz-magnetite-chalcopyrite) is found within the gabbro-diorite both in Tak I and Tak II, but the granodiorite is cutting the mineralized rocks. This is also a good evidence that gabbro-diorite is older than granodiorite-granite. It has porphyry texture. It contains 55% plagioclase and 40% pyroxene (aegirine-augite). Due to regional metamorphism and alteration both plagioclase and pyroxene are altered to chlorite and carbonate.

Spotted granite: It crops out only in Tak-II (Fig. 3). It has porphyry textures with elongated black ellipsoids (Figs. 5, 6). These elongated ellipsoids formed during regional metamorphism and along the fault movements. The ellipsoids are consist of chlorite, quartz & opaque minerals.

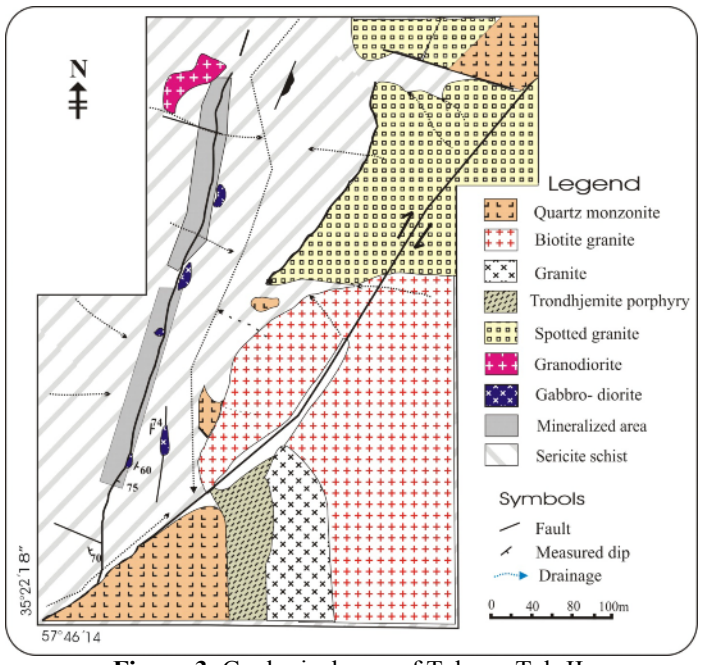

Figure 3. Geological map of Taknar, Tak-II.

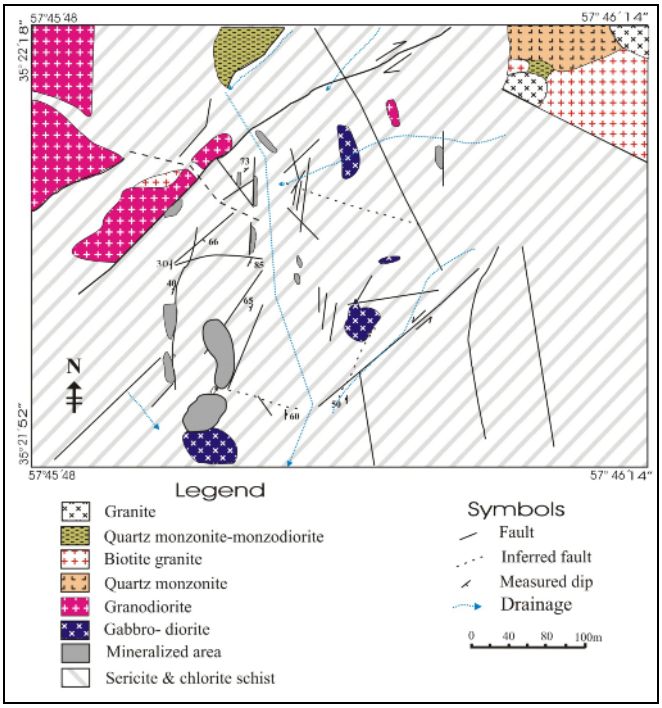

Figure 4. Geological map of Taknar, Tak-I.

Figure 5. Field photograph of spotted granite showing elongated ellipsoid.

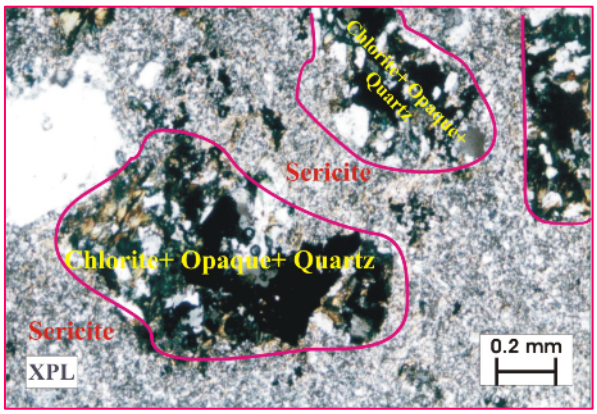

Figure 6. Photomicrograph of spotted granite showing that the spots are consisted of opaque minerals, chlorite and quartz.

Analytical Results

Whole-rock geochemistry

Representative rocks from the Bornaward (Taknar) granitoid were analyzed for major and trace elements (Table 1). Chemical composition of Bornaward (Taknar) granitoid rocks were plotted in TAS diagram [14], and they fall into the fields of granite and granodiorite (Fig. 7). Villaseca [15] divided per-aluminous granites into four groups (Fig. 8): (1) Highly per-aluminous granitoids (H-P), which are the typical S-type granites. They have the highest A = (Al/(K + Na +2Ca). They are characterized by having Al-rich minerals such as muscovite, garnet (almandine-pyrope series), cordierite, and sillimanite. They usually contain abundant restitic enclaves. (2) Moderately per-aluminous granitoids (M-P). These are biotite bearing. Accessory phases are cordierite and garnet (almandine-spessartine series). (3) Low per-aluminous granitoids (L-P). These rocks could be evolved from I-type or low-ASI-type granitoids. They may contain amphibole. Enclaves are mainly mafic granular types. (4) Highly felsic per-aluminous granitoids (F-P).

Bornaward (Taknar) granite and granodiorite plot in the field of highly per-aluminous (m-P) and met-aluminous granitoids (h-P) (Fig. 8). The granitic rocks are medium- to high-potassic (Fig. 9).

Chemical composition of Bornaward (Taknar) granitoid rocks are plotted in Ga/Al- vs. trace element discrimination diagrams [18]. They plot in the field of I & S- type granites (Fig. 10).

Table 1. Major and trace elemental analysis of Bornaward granitoid.

Sample Location	TK2-8	TK1-5	Tk2-18	Tk1-48	Tk2-35	TK2-29	TK2-15	TK2-18
SiO_2	71.37	72.68	76	69.77	71.55	71.61	71.48	70.8
TiO_2	0.13	0.26	0.1	0.17	0.17	0.16	0.19	0.16
Al_2O_3	12.68	12.73	10.93	13.29	13.66	12.06	12.61	13
Fe_2O_3	1.63	1.76	1.6	1.67	1.67	1.66	1.69	1.66
FeO	2.78	1.49	1.08	2.73	2.49	2.12	3.09	2.6
MnO	0.03	0.05	0.01	0.06	0.04	0.03	0.04	0.02
MgO	0.11	1.63	0.06	1.52	0.62	1.32	0.34	0.42
CaO	0.46	0.8	0.89	0.41	0.87	1.02	0.36	0.48
Na_2O	4.42	2.76	0.28	2.69	1.4	2.66	2.04	4.69
K_2O	2.98	3.04	5.83	4.45	3.36	3.71	4.99	3.49
P_2O_5	0.06	0.06	0.06	0.08	0.06	0.04	0.08	0.07
Rb	66.8	142.1	107	134.2	91.7	127.3	124.3	130.4
Sr	54.6	40	36.8	55.1	66.9	110.9	53.6	65.1
Ba	495	622	1656	1755	1311	1299	1974	981
Nb	11.3	12.6	8.9	10.6	10.8	10.6	10.5	11.4
Zr	166.4	214.4	116.2	170.9	164.2	137.7	167.8	168.9

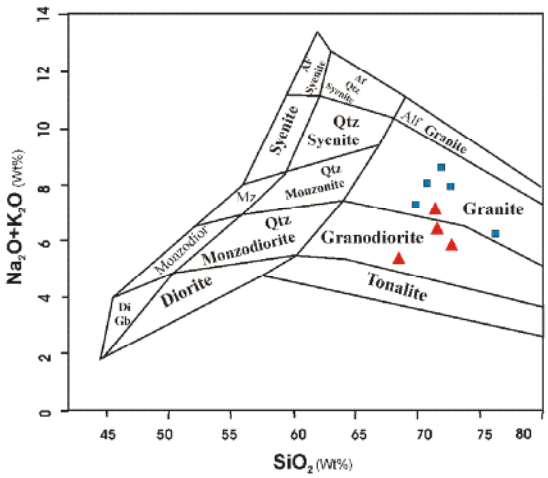

Figure 7. Composition of Bornaward (Taknar) granitoid plotted on the TAS diagram [14].

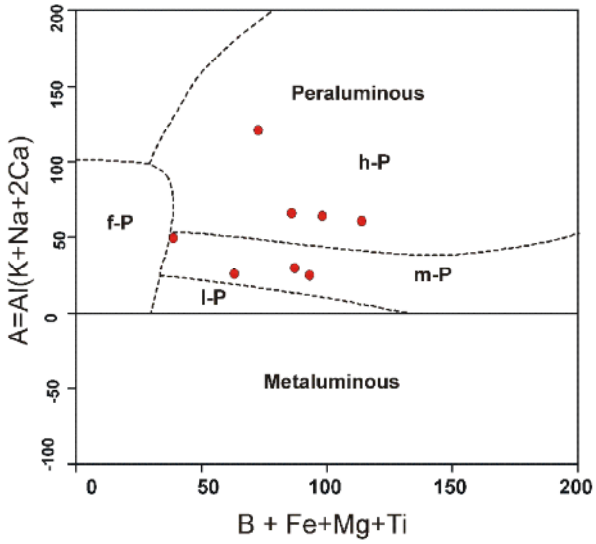

Figure 8. Composition of Bornaward (Taknar) granitoid plotted on Villaseca [15] diagram. Bornaward (Taknar) granite and granodiorite plot in the fields of moderately peraluminous (M-P) and high peraluminous. (L-P = low peraluminous; M-P = moderately peraluminous; H-P = highly peraluminous; F-P = felsic peraluminous).

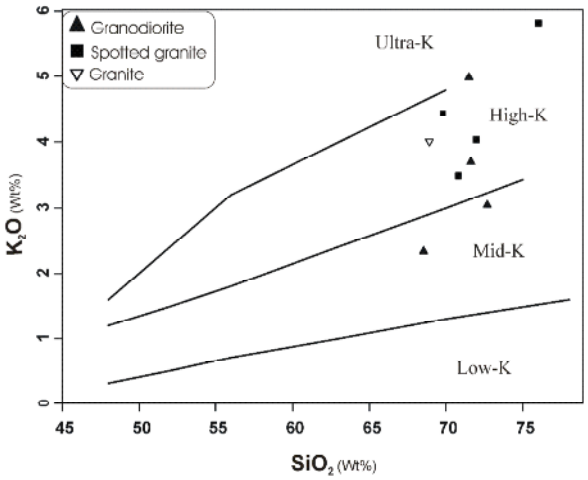

Figure 9. K_2O vs. SiO_2 variation diagram [16] with boundaries by [17] for high-K, medium-K, and low-K magma series.

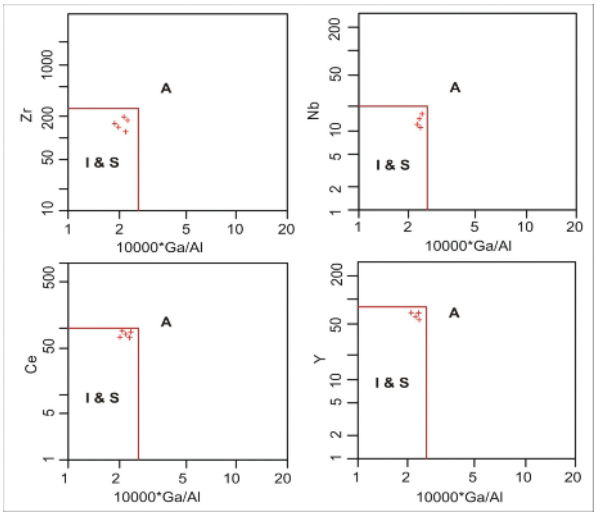

Figure 10. Bornaward granitoid are plotted in the field of I & S type [18].

Compositions of granitic rocks from the Bornaward plotted on the CaO/Na_2O– Al_2O_3/TiO_2 diagram. The field of S-granites and its boundaries are given after [19]. Bornaward granitoid plot in the field of S –type granite (Fig. 11). Representative rock samples from Bornaward granite and granodiorite were analyzed for rare earth and trace elements using ICP-MS at the ACME Lab (Canada) (Table 2). REE from Dehnow S-Type Paleo-Tethys granitoids (Mashhad) and Najmabad granitoids (Ghonabad) (both S and I –type's granitoids) are presented in Table 2 [20, 21]. Lower continental crust-normalized trace-element diagrams indicates that both granite and granodiorite are relatively enriched in LILE = Rb, K and depleted in Cs, Ba, Nb, Ta, Sr (Fig. 12). In comparison with granodiorite (S-type) from Dehnow and Najmabad, Bornaward granitoids show very strong depletion in Sr and Ti (Fig. 12).

Chondrite-normalized rare earth element (REE) plots indicate minor enrichments of light relative to heavy REE, with $(La/Yb)_N$ between 3.5-5.6 (Fig. 13) and high total REE = 193-252 with strong negative anomaly of Eu (Fig. 13). Dehnow and Najmabad granodiorite have $(La/Yb)_N$ = 7 to 22 and no, or only small, negative Eu anomalies (Eu/Eu* = 0.55 to 1.1) (Fig. 13).

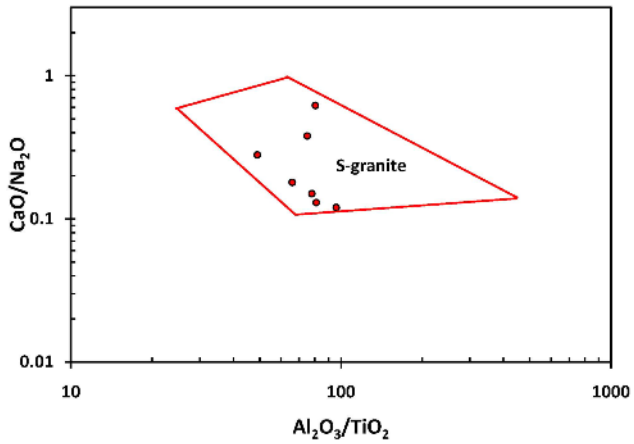

Figure 11. Compositions of granitic rocks from the Bornaward plotted on the CaO/Na_2O– Al_2O_3/TiO_2 diagram. The field of S-granites and its boundaries types are given after [19].Bornaward granitoids are plotted in the field of S –type granite.

Table 2. REE elements analysis of Bornaward, Dehnow and Najmabad intrusive rocks [20, 21].

Location	Sample	La	Ce	Pr	Nd	Sm	Eu	Gd	Tb	Dy	Ho	Er	Tm	Yb	Lu
Bornaward	Tk2-18 Granite	42.1	82.6	8.7	33.3	7.18	0.64	7.59	1.58	10.04	2.05	6.13	0.78	5.45	0.77
Bornaward	Tk1-48 Granite	32.6	79.8	8.67	34	7.03	0.76	7.17	1.38	8.32	1.79	5.38	0.7	5.03	0.75
Bornaward	Tk2-8 Granite	46.2	99.3	11.91	46.8	9.61	1.05	8.79	1.5	9.12	1.84	5.71	0.77	5.51	0.78
Bornaward	Tk2-35 Granite	44.7	99.1	11.98	45.3	10.05	0.97	10.15	1.88	11.18	2.2	6.42	0.85	6.16	0.85
Bornaward	Tk1-5 granodiorite	36.1	79.2	9.48	35.2	8.24	0.92	8.89	1.81	11.71	2.45	7.37	0.94	6.98	0.96
Dehnow	Granodiorite	37	78.2	8.31	29.6	5.12	1.27	3.86	0.55	2.61	0.48	1.22	0.18	1.17	0.17
Dehnow	Granodiorite	37.2	79	8.11	30.7	5.26	1.3	4.37	0.69	3.72	0.69	1.97	0.29	1.95	0.3
Najmabad	KC-119 Granodiorite	29.7	64.9	7.3	27.3	5.39	0.96	4.81	0.79	4.51	0.84	2.52	0.32	2.44	0.36
Najmabad	KC-127 Granodiorite	22.6	49.1	5.52	21.9	4.07	0.92	3.43	0.56	3.23	0.62	1.83	0.22	1.73	0.25
Najmabad	KP-3 Monzonite	13.6	28.7	3.61	13.9	2.63	0.86	2.1	0.29	1.34	0.23	0.6	0.07	0.55	0.08
Najmabad	KP-2 Monzonite	16.5	37.8	4.57	18.1	2.98	0.85	2.2	0.28	1.33	0.21	0.56	0.06	0.5	0.06
Najmabad	KP-25 Monzonite	16.9	37.1	4.36	16.8	2.9	0.82	2.04	0.27	1.33	0.21	0.63	0.07	0.53	0.08

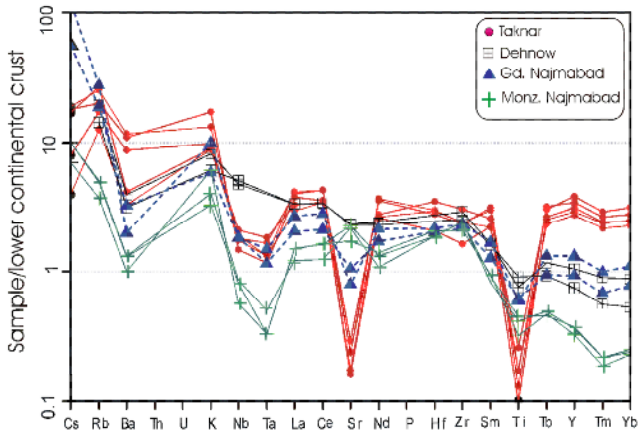

Figure 12. Spider diagram for Bornaward, Dehnow, and Najmabad intrusive. Data for Lower continental crust are from [22].

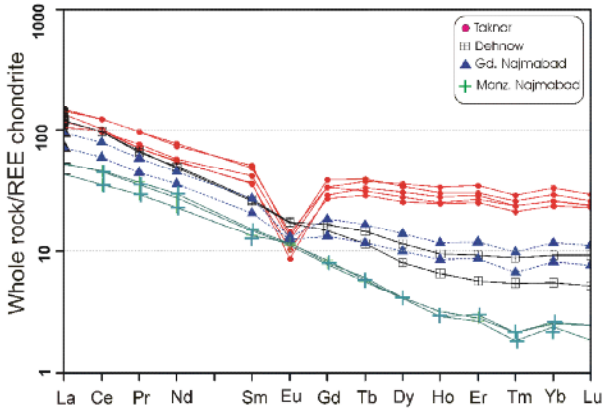

Figure 13. Chondrite-normalized REE distribution [23] for Bornaward granite and granodiorite.

Magnetic susceptibility

Granitic rocks were classified into the magnetite series and the ilmenite series by Ishihara (1977). Ishihara recognized that in Japan there is a distinct spatial distribution of granitic rocks that contain magnetite coexisting with ilmenite and those that contain ilmenite as the only Fe-Ti oxide. He recognized that the magnetite-series granitoids are relatively oxidized, whereas the ilmenite-series granitoids are relatively reduced. Granites showing a magnetic susceptibility value of $>3.0 \times 10^{-3}$ (SI units) are classified as belonging to the magnetite series [24]. Magnetic susceptibility ($<3.0 \times 10^{-3}$ (SI units) and mineralogical composition of the studied granite and granodiorite indicate that they belong to the ilmenite series.

U-Th-Pb Zircon age dating

The age of Taknar Formation and the granitoid rocks (Bornaward) are becoming an interesting subject. Based on field observation, Muller and Walter [1] suggested that Taknar Formation is Precambrian in age. Recent Palynological studies show that the age of Taknar Formation is Ordovician [4]. Using the Rb–Sr whole-rock and biotite isotopic methods by Soltani [5] on granitoid rocks (Bornaward granite) gave values of 154 to 111 Ma. The initial ($^{87}Sr/^{86}Sr$) > 0.76 for the granitoid based on Soltani [5] is very high and unusual. It became interested to find out the accurate age of Taknar Formation and the granitoids. We used more accurate U-Pb in zircon age dating.

Two rock samples, which were analyzed for Sr and Nd isotopes (granodiorite-granite), were chosen for U-Pb-Th dating of Zircon. The U-Th-Pb dating of Zircon was done at Department of Geosciences University of Arizona Tucson, (USA).

The results of U-Th-Pb zircon analysis of the two samples No TAK2-8 and TAK1-5 are presented in the Table (3). The results of calculation of isotopic (sample no TAK2-8, granite) age is presented in the TuffZirc diagram (Fig. 12). The zircon sample TAK2-8 (granite) (Fig. 12) has 12 analyzed points giving the mean

age value (weighted mean) of 552.69 ± 10.89 Ma (error in the 2 sigma level). The results of calculation of isotopic (sample TAK1-5, granodiorite) age are presented in the TuffZirc graphics (Fig. 13). Based on 32 analyzed points the mean age value (weighted mean)for granodiorite is 538.22 – 1.82, + 4.28 Ma (error in the 2 sigma level).

Based on U-Th-Pb zircon age dating, Bornaward granite and granodiorite were formed in late Neoproterozoic time.(Fig 14, 15)

Table 3. Results of U-Pb-Th laser-ablation multicollector ICP mass spectrometry analysis of zircon from Bornaward granite and granodiorite.

Analysis	U (ppm)	206Pb/204Pb	U/Th	206Pb/207Pb	± (%)	207Pb/235U	± (%)	206Pb/238U	± (%)	Age (Ma)	± (Ma)
TAK2-8-1C	376	24213	1.7	16.7772	1.5	0.7202	1.8	0.0876	1.0	541.5	5.1
TAK2-8-2C	245	18913	1.7	17.1670	3.4	0.7116	3.8	0.0886	1.6	547.2	8.3
TAK2-8-3C	263	20831	1.8	17.2811	3.3	0.7157	3.4	0.0897	0.9	553.8	4.9
TAK2-8-5C	541	44610	2.0	17.2002	1.9	0.7017	2.6	0.0875	1.8	540.9	9.5
TAK2-8-6T	429	37871	2.0	17.2354	1.2	0.7309	1.8	0.0914	1.3	563.6	6.8
TAK2-8-7T	497	41350	1.9	17.2885	1.1	0.7139	2.1	0.0895	1.9	552.7	9.8
TAK2-8-8C	422	21395	1.7	17.0230	1.4	0.6743	1.9	0.0832	1.3	515.5	6.6
TAK2-8-9C	146	54031	1.9	16.8001	4.7	0.7065	9.9	0.0861	8.7	532.3	44.3
TAK2-8-10C	289	61030	1.5	16.9000	3.0	0.7350	3.4	0.0901	1.6	556.0	8.4
TAK2-8-12C	725	52668	1.3	17.0615	1.0	0.6883	1.3	0.0852	0.9	526.9	4.5
TAK1-5-1C	432	45846	3.4	14.9263	0.8	1.2464	1.7	0.1349	1.5	815.9	11.1
TAK1-5-2C	461	40369	2.1	16.9605	1.4	0.7346	1.4	0.0904	0.3	557.7	1.8
TAK1-5-3T	305	34228	2.3	17.3272	2.8	0.6938	2.9	0.0872	0.7	538.9	3.8
TAK1-5-4T	628	21930	2.8	17.0480	1.5	0.6695	1.7	0.0828	0.7	512.7	3.6
TAK1-5-5C	564	99521	1.1	13.9042	0.6	1.6024	4.0	0.1616	4.0	983.7	11.9
TAK1-5-6T	1071	94482	2.9	16.4676	0.9	0.8479	1.8	0.1013	1.6	621.9	9.6
TAK1-5-7C	448	30356	3.1	17.0575	1.2	0.6981	1.7	0.0864	1.2	534.0	6.0
TAK1-5-8C	360	33821	3.7	16.8601	1.4	0.7605	4.9	0.0930	4.7	573.2	25.7
TAK1-5-9C	1202	112969	2.0	17.0753	0.4	0.6973	1.4	0.0864	1.3	533.9	6.7
TAK1-5-10C	529	35368	3.8	16.9637	0.7	0.6901	1.4	0.0849	1.1	525.3	5.7
TAK1-5-11C	290	21759	4.1	17.0125	3.2	0.6766	3.4	0.0835	1.3	516.9	6.6
TAK1-5-12T	329	33909	3.5	17.0886	1.4	0.7222	1.7	0.0895	1.0	552.6	5.2
TAK1-5-13T	446	42534	2.6	17.0743	1.3	0.7181	2.0	0.0889	1.5	549.2	7.8
TAK1-5-14T	938	61488	2.7	16.8978	0.7	0.7317	2.5	0.0897	2.4	553.6	12.7
TAK1-5-16T	271	15615	1.7	16.6030	4.0	0.7184	4.9	0.0865	2.8	534.8	14.2
TAK1-5-17T	542	40302	1.6	16.8853	1.2	0.6911	2.5	0.0846	2.2	523.7	11.3
TAK1-5-18C	510	34756	1.3	16.9926	1.3	0.7133	1.5	0.0879	0.8	543.2	4.4
TAK1-5-19T	376	30795	2.1	17.0282	2.2	0.7159	3.9	0.0884	3.2	546.1	16.8
TAK1-5-20T	258	27504	2.1	17.3455	1.4	0.6987	1.7	0.0879	0.9	543.1	4.7
TAK1-5-21T	400	26329	3.1	16.7358	2.8	0.7597	3.5	0.0922	2.1	568.6	11.2
TAK1-5-22T	313	23018	1.6	17.0354	2.3	0.7057	4.8	0.0872	4.2	538.9	21.9
TAK1-5-23T	738	67172	1.4	17.0728	0.9	0.7057	1.4	0.0874	1.1	540.0	5.6
TAK1-5-24T	481	53142	2.4	17.0398	0.9	0.7065	1.6	0.0873	1.3	539.7	6.9
TAK1-5-25T	227	19898	2.8	16.8117	2.1	0.7082	2.8	0.0864	1.9	533.9	9.7
TAK1-5-27T	335	11428	3.3	16.6330	5.4	0.7209	5.5	0.0870	0.7	537.6	3.4
TAK1-5-28T	573	27325	1.7	16.9589	1.3	0.7047	2.4	0.0867	2.0	535.8	10.3
TAK1-5-29T	258	31373	1.9	16.3340	1.2	0.8920	2.4	0.1057	2.1	647.6	12.6
TAK1-5-30T	613	18086	1.7	16.8825	1.6	0.7123	2.7	0.0872	2.2	539.1	11.3
TAK1-5-31T	412	35728	2.9	16.9675	2.0	0.6992	2.9	0.0860	2.0	532.1	10.3
TAK1-5-32T	421	23796	4.0	16.7739	1.5	0.6941	2.4	0.0844	1.9	522.5	9.7

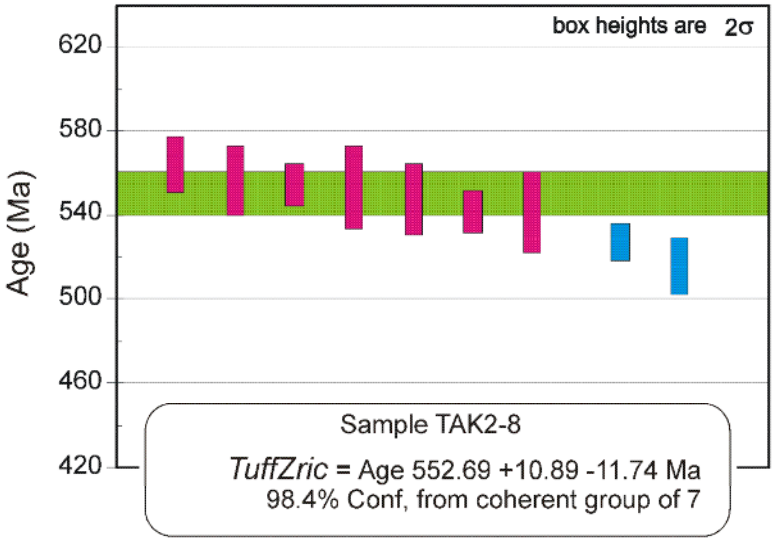

Figure 14. TuffZirc graphics for calculating the age of zircons (TAK2-8).

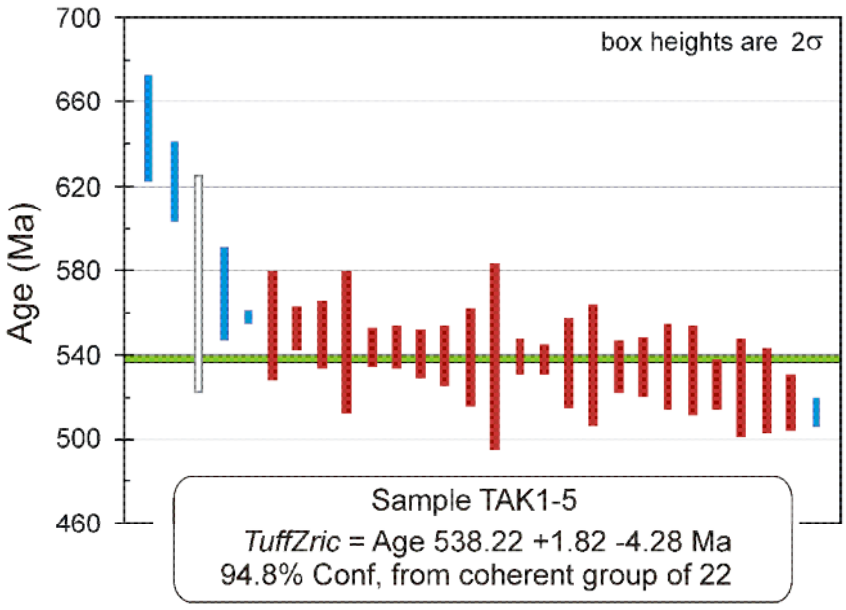

Figure 15. TuffZirc graphics calculating the age of zircons (TAK1-5).

Sr–Nd IsOtopes

Sr and Nd isotope data for representative samples are given in Table (4). They have a range in initial $^{87}Sr/^{86}Sr$ and $^{143}Nd/^{144}Nd$ from 0.713566 to 0.716888 and 0.511791 to 0.511842, respectively, when recalculated to an age of 553 and 538 Ma, they are consistent with the new radiometric results (Table 4). Initial εNd isotope values for granite and granodiorite range from -2.62 to -2.01 (Table 4).

Soltani [5] analyzed several plutonic rocks between Torbat-Hydarieh, Drouneh and Sabzevar for Rb-Sr. The result of his study only for two localities, Bornaward (Taknar) and Kashmar are presented in Table (5). Based on field data and Rb-Sr age, the Kashmar granitoid formed in Tertiary. The initial ($^{87}Sr/^{86}Sr$) is between 0.7048 to 0.7056 and the age is 42 Ma (Table 5). The initial ($^{87}Sr/^{86}Sr$) for Bornaward granitoid is between o.71637 to 0.7500 and the age is 152.8 to 111.8 Ma (Table 5). The age which was calculated based on Rb-Sr in whole rock and biotite is incorrect (Table 5). Since the age was incorrect therefore the initial ($^{87}Sr/^{86}Sr$) is incorrect too.

Table 4a. Rb-Sr isotopic composition of Bornaward granite and granodiorite

Sample	Rb (ppm)	Sr (ppm)	$^{87}Rb/^{86}Sr$	$(^{87}Sr/^{86}Sr)m$ (2σ)	R0(Sr)
Granodiorite TK1-5	111	50	6.0167	0.766090 (9)	0.716888
Granite TK2-8	41	79	1.4999	0.725390 (1)	0.713566

Table 4b. Sm-Nd isotopic composition of Bornaward granite and granodiorite

Sample	Sm (ppm)	Nd (ppm)	$^{147}Sm/^{144}Nd$	$(^{143}Nd/^{144}Nd)m$ (2σ)	R0(Nd)	εNd I	T_{DM}
Granodiorite TK1-5	6.18	27	0.1385	0.512330 (12)	0.511842	-2.01	1.44
Granite TK2-8	7.7	36	0.1294	0.512260 (09)	0.511791	-2.62	1.41

m= measured. Errors are reported as 2σ (95% confidence limit).
R0(Sr) is the initial ratio of $^{87}Sr/^{86}Sr$ for each sample, calculated using $^{87}Rb/^{86}Sr$ and $(^{87}Sr/^{86}Sr)m$ and an age of 538 Ma (granodiorite) and 553 Ma (granite) (age based on zircon).
R0(Nd) is the initial ratio of $^{143}Nd/^{144}Nd$ for each sample, calculated using $^{147}Sm/^{144}Nd$ and $(^{143}Nd/^{144}Nd)m$ and an age of 538 Ma (granodiorite) and 553 Ma (granite) (age based on zircon).
εNdI, initial εNd value.

Table 5. Rb-Sr and Age of Bornaward (Taknar) and Kashmar granite [5]

	Bornaward (Taknar) Granite						
Sample	Rock	Rb	Sr	$^{87}Rb/^{86}Sr$	$(^{87}Sr/^{86}Sr)m$	$(^{87}Sr/^{86}Sr)i$	Age Ma
R15947	Granodiorite	70	109	1.904	0.72050	0.71637	152.8 ±1.3
	Biotite	622	14.84	124.633	0.98700		
R15946	Granodiorite	129	145	2.641	0.72700	0.72153	145.6±1.3
	Biotite	635	13	148.788	1.02937		
R15938	granite	95	39	7.246	0.75253	0.73978	123.8±1
	biotite	947	11	258.519	1.19453		
R15941	granite	128	39	9.775	0.76562	0.75008	111.8±1.1
	biotite	715	16.17	130.959	0.95823		
Sample	Rock	Rb	Sr	$^{87}Rb/^{86}Sr$	$(^{87}Sr/^{86}Sr)m$	$(^{87}Sr/^{86}Sr)i$	Age Ma
R15915	Granodiorite	62	273	0.672	0.70610	0.70569	42.8±0.5
	Biotite	346	23.3	43.115	0.73193		
R15910	Granite	103	315	0.968	0.70574	0.70516	42.4±0.4
	Biotite	440	7.9	162.759	0.80313		
R15918	Granite	88	288	1.382	0.70615	0.70532	42.5±0.5
	biotite	397	14.4	77.998	0.75235		
R15900	Alkali feldspar granite	200	50	11.83	0.71209	0.70478	43.5±0.4
	biotite	689.8	4.53	16.99	0.71504		

Dscussion section

Surce of Magma

Based on mineralogy and low values of magnetic susceptibility [(5 to 11) × 10^{-5} SI], both granite and granodiorite are classified as belonging to the ilmenite-series of reduced S-type granitoids. Chemically they are per-aluminous, high-K calc-alkaline with relative enrichment in LILE, Rb, K and depletion in Sr, Ba, Nb, Ti, Ta, Y, Yb. Chondrite-normalized rare earth element (REE) plots indicate minor enrichments of light relative to heavy REE, with $(La/Yb)_N$ between 3.5-5.6. They show high total REE = 193-252 with strong negative anomaly of Eu.

Initial $^{87}Sr/^{86}Sr$, εNd and $^{143}Nd/^{144}Nd$ of MORB basalts, Bornaward Granite-granodiorite and Dehnow diorite-granodiorite are plotted in Fig. 16. Initial $^{87}Sr/^{86}Sr$ isotope values for Bornaward Granite-granodiorite range from 0.713566 to 0.716888, Dehnow diorite- granodiorite range from 0.707949 to 0.708589 and MORB is less than 0.7040. Initial $^{143}Nd/^{144}Nd$ isotope values for Bornaward Granite-granodiorite range from 0.511842-0.511791, Dehnow diorite - granodiorite range from 0.512059–0.512019 and for MORB is between 0.5130 to 0.5135. Both Bornaward and Dehnow granitoid are originated from the continental crust. The Initial $^{87}Sr/^{86}Sr$ isotope values for Bornaward Granite-granodiorite

(0.713566) is much higher than Dehnow granodiorite (0.708). This indicates the source of magma for Bornaward Granite-granodiorite was originated from the continental crust and is was more radiogenic.

Samarium-neodymium T_{DM}'s can provide an estimate for the time at which continental crust was extracted from a depleted mantle source. Therefore, T_{DM} ages may delineate crustal blocks of differing ages [25-27]. Granite and granodiorite of Bornaward yields a T_{DM} age of 1.4-1.41 Ga (Table 4b). This indicates that the granites and granodiorite being derived from partial melting of distinct basement source regions.

The Rb/Sr versus Rb/Ba discrimination diagram (Fig. 17) shows that Bornaward granitoid rocks plot next to metapelitic derived melt [19]. Dehydration-melting behavior of biotite in metapelitic rocks has been investigated by many workers, including [28-36]. The amount and composition of melts produced is dependent on different factors: composition of the source rocks, temperature, water, pressure and oxygen fugacity. In general, as the melt produced at low melting fractions are indistinguishable (mainly per-aluminous), irrespective of the nature of the protolith only the amount of melt will be different. Even metaaluminous meta-igneous rocks such those reported by [37-41] are able to produce per-aluminous felsic melts at low melting fractions and in water-deficient conditions. As the melting increases, primary component of the source rocks are progressively incorporated in the melt. The Ti and Mg content of biotite directly control the reaction temperature interval in biotite. As these elements increase in biotite, the reaction temperature interval will expand.

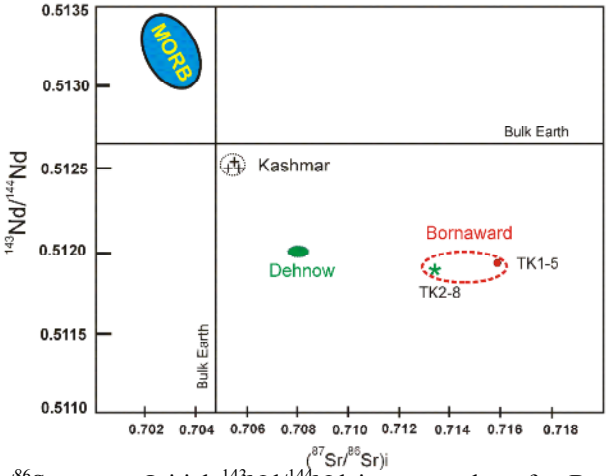

Figure 16. Plot of Initial $^{87}Sr/^{86}Sr$ versus Initial $^{143}Nd/^{144}Nd$ isotope values for Bornaward, Dehnow and Kashmar granitoid rocks.

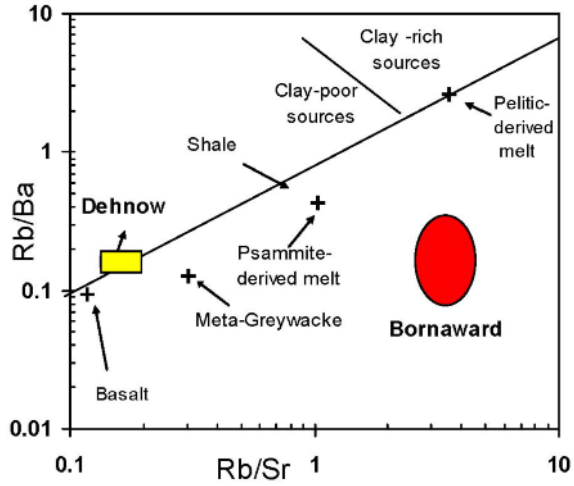

Figure 17. Plot of Rb/Sr versus Rb/Ba, Bornaward granitoid plot in the field near politic rock but Dehnow granitoid plot in the field near meta-greywacke.

Late Neoproterozoic granitoid rocks in Iran

Results of study by Hassanzadeh [42] demonstrate that Late Neoproterozoic to Early Cambrian granitoids and granitic gneisses are present in all continental structural zones of Iran north of the Zagros, from the Sanandaj–Sirjan zone to the northern margin of the Alborz Mountains (Table 6). Therefore, the crystalline basement of Iran can be considered to be the approximate northern continuation of the Arabian platform [42]. Since definitive crust of comparable age is generally absent in cratonic Eurasia [43], the occurrences of granitoids with Neoproterozoic ages from the Zagros to the northern foothills of the Alborz point to a Gondwana affinity for the continental terrains composing Iran.

Granitoid rocks of Late Neoproterozoic age are exposed in Saghand region (central Iran) [44]. Two multi-grain and one single-grain zircon fractions from a Boneh-Shurow (Saghand region) quartz-diorite intrusion yielded concordant analyses with an average $^{207}Pb/^{206}Pb$ age of 547.6 ± 2.5 Ma [44] (Fig. 18). Figure (18) show the distribution of Late Neoproterozoic granitoid rocks in Iran.

Conclusions

Taknar zone is an exotic block bordered with two major faults, Great Kavir fault (Drouneh) to the south and Rivash fault in the north. Taknar Formation is divided into lower, middle and upper members. It consists of meta-tuff, meta-rhyolite, slate, chlorite schist and quartzite.

A complex of intrusive rocks crop out at the center of Taknar zone. They are named as "Bornaward granite". The intrusive rocks are composed of granite, granodiorite, monzonite and diorite. Granite and granodiorite are dominant. Based on field observation diorite is older than granite and granodiorite.

Table 6. Thermal-ionization (TIMS) zircon U-Pb geochronology [42].

Region	Area	Age Ma U-Pb Zircon
Northwest Iran	Sarv-e Jahan granite	544±29 Ma 599±42 Ma
	Doran granite	567±19 Ma
Takab-west Zanjan area	Moghanlou granite	548±27 Ma
	Mahneshan granitoid complex	568±44 Ma
Northwestern Sanandaj–Sirjan zone	Sheikh Chupan granodiorite	551±25 Ma
	Bubaktan	544±19Ma
Golpaygan area	Muteh Au mine	578±22 Ma
Northeast central Iran	Torud granite	566±31 Ma
	Khār Turan granite	554±40 Ma
	Band-e Hezar Chāh granite	581±21 Ma
Northern Alborz	Lahijan granite	551±9 Ma

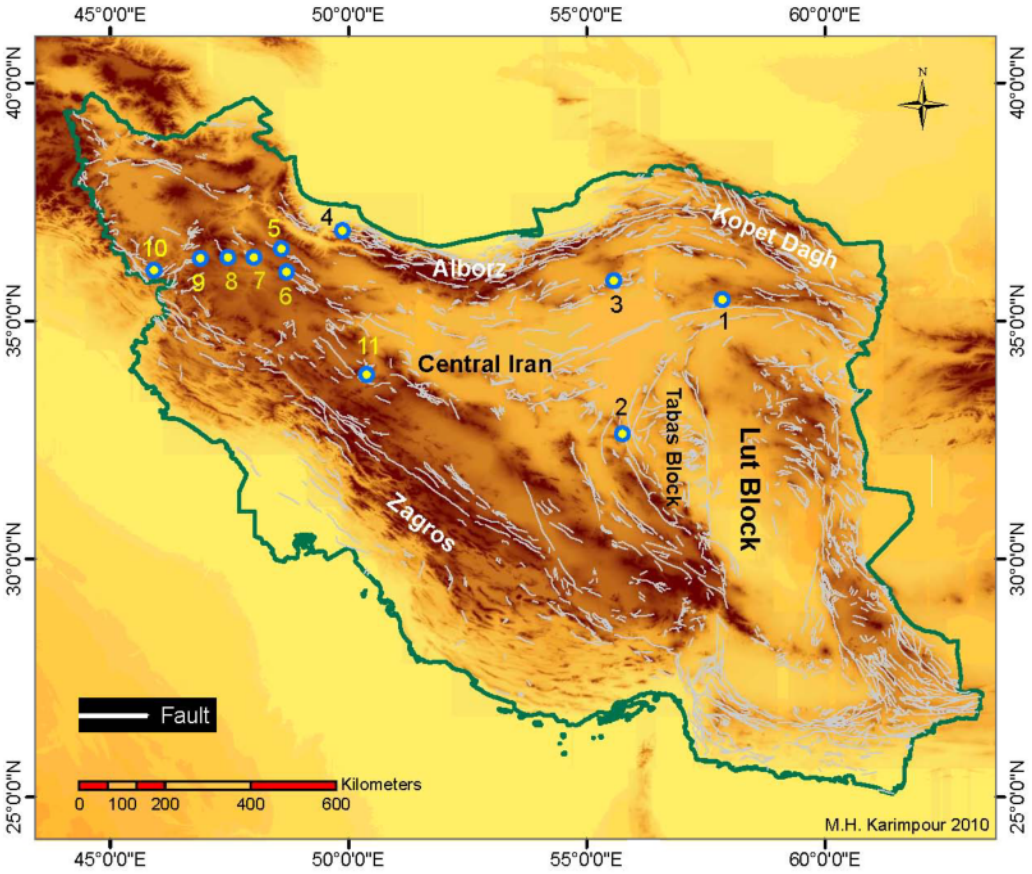

Figure. 18. Map shows the location of Late Neoproterozoic granitoid rocks in Iran

1-Bornaward; 2- Saghand; 3- Khār Turan, Band-e Hezar Chāh, Torud; 4- Lahijan granite; 5- Khorram Darreh; 6- Sarv-e Jahan; 7- Doran; 8- Mahneshan; 9- Moghanlou; 10- Bubaktan, Sheikh Chupan; 11- Mouteh.

Both granite and granodiorite are classified as belonging to the ilmenite-series of reduced S-type granitoids. Chemically they are per-aluminous, high-K calc-alkaline with relative enrichment in LILE = Rb, K and depletion in Sr, Ba, Nb, Ti, Ta, Y, Yb. Chondrite-normalized rare earth element (REE) plots indicate minor enrichments of light relative to heavy REE, with $(La/Yb)_N$ between 3.5-5.6. High total REE = 193-252 with strong negative anomaly of Eu.

The results of U-Pb zircon age of granodiorite is 552.69 ± 10.89 Ma and granite is 538.22 – 1.82, + 4.28 Ma (late Neoproterozoic time). They have a range in initial $^{87}Sr/^{86}Sr$ and $^{143}Nd/^{144}Nd$ from 0.713566 to 0.716888 and 0.511791 to 0.511842, respectively, when recalculated to an age of 553 and 538 Ma, consistent with the new radiometric results. Initial εNd isotope values for granite and granodiorite range from -2.62 to -2.01.

Granite and granodiorite of Bornaward yields a T_{DM} age of 1.4-1.41 Ga. This indicates that the granites and granodiorite being derived from partial melting of distinct basement source regions with very high initial $^{87}Sr/^{86}Sr$.

Bornaward and other Late Neoproterozoic granitoid rocks which are exposed and are dated until today are located along the margin of central Iran plate. Knowing the petrogenesis and tectonic setting of all of these granitoids will help to understand the relationship between Gondwana and central Iran plate.

Acknowledgements

This research was supported by Ferdowsi University of Mashhad, Iran (grant P/1724-

86/11/28). George E. Gehrels and Victor Valencia from Department of Geosciences University of Arizona Tucson did the U-Th-Pb Zircon age dating. From department of Geological sciences at CU Boulder, Special thanks to Emily Verplanck for her help in obtaining the isotopic data for this study.

References

[1] Muller R., Walter R. *"Geology of the Precambrian-Paleozoic Taknar inliers northwest of Kashmar, Khorasan province, NE Iran"*, GSI. Rep. No. 51, (1983)165-183.

[2] Lindenberg H.G., Jacobshagen V., *"Post-Paleozoic geology of the Taknar zone and adjacent area, NE Iran, Khorasan"*, GSI. Rep. No. 51, (1983) 145-163.

[3] Eftekharnejad J., Aghanabati A., Baroyant V., Hamzehpour B., *"Geological Map of Kashmar, 1: 250000"*. GSI, Tehran (1976).

[4] Personal Conversation with Dr Ghavidel, M *"concerning the age of Taknar Formation using Palynology"* (2003).

[5] Soltani A., *"Geochemistry and geochronology of I–type granitoid rocks in the northeastern Central Iran Plate"*. PhD Thesis, University of Wollongong, Australia (unpubl.), (2000) 300 p.

[6] Razzaghmanesh B., *"Die Kupfer- Blei- Zink-Erzlagerstatten von Taknar und ihr geologischer Rahmen (NE- Iran)"*. Diss. Aachen, 131 p, Aachen (1958).

[7] Forster H., *"Associations of volcanic rocks in the mountains South of Sabzevar (NE Iran"*, 23. IGK. 2: (1968) 197- 212, Montreal.

[8] Karimpour M.H., Malekzadeh A., *"Petrography of intrusive rocks, mineralogy of altered rocks formed at different stages, and the effect of both regional and contact metamorphism at Tak-II (Taknar mine Khorasan, Iran)",* Proceedings of the 11th Symposium of Society of Crystallography and Mineralogy of Iran, University of Yazd, (2004) 209-214.

[9] Homam S.M., *"Geology and petrology of Taknar Formation, Northwest of Kashmar, Khorasan Razavi Province"*, M.Sc. Thesis, University of Esfahan, (1992) 126 .

[10] Sepahigrou A.A., *"Petrology of granitoid rocks of Taknar- Sarborj, Northwest of Kashmar, Khorasan Razavi Province"*, M.Sc. Thesis, University of Esfahan, (1992) 126 p.

[11] Zijanizadeh S., *"petrology of intrusive rocks, microthermometry and stable isotopes study of Taknar polymetal massive sulfide"*, M.Sc. thesis, Ferdowsi University of Mashhad (2008) 186p.

[12] Malekzadeh A., Geology, *"mineralogy and geochemistry of Taknar polymetal (Cu-Zn-Au-Ag-Pb) deposit (Tak-I & II) and determining type of mineralization"*, M.Sc. Thesis, Ferdowsi University of Mashhad,(2004) 287p .

[13] Ghoorchi M., *"Geology, mineralogy and geochemistry of Taknar deposit (Tak-III & IV), Bardaskan"*, M.Sc. Thesis, Ferdowsi University of Mashhad, (2004) 219 p.

[14] Middlemost Eric A. K., *"Naming materials in the magma igneous rock system"*, Earth Sci, Rev., 37 (3-4): (1994) 215-224.

[15] Villaseca C., Barbero L., Herreros V., *"A re-examination of the typology of peraluminous granite types in intra continental orogenic belts"*, Transactions of the Royal Society of Edinburgh: Earth Sciences 89, (1998) 113–119.

[16] Rickwood P.C., *"Boundary lines within petrologic diagrams which use oxides of major and minor elements. Lithos 22"*, (1989) 247–267.

[17] Peccerillo A., S.R. Taylor, *"Geochemistry of Eocene calc-alkaline volcanic rocks from the Kastamonu area, Northern Turkey"*. Contributions to Mineralogy and Petrology 58, (1976) 63–81.

[18] Whalen J B, Currie K L, Chappell BW., *"A-type granites: geochemical characteristics, discrimination and Petrogenesis"*, Contrib Mineral Petrol 95: (1987) 407-419.

[19] Sylvester P.J. *"Post-Collisional Strongly Peraluminous Granites,"* Lithos 45, (1998) 29–44.

[20] Karimpour M.H., Stern C. R., L. Farmer, *"U-Pb-Th (zircon) Geochronology, Rb-Sr & Sm-Nd Isotopic Composition and Petrogenesis of Dehnow Kuhsangi Paleo-Tethys Diorite-Granodiorite, Mashhad, Iran",* Journal of Asian Earth Sciences 37: (2010) 384-393.

[21] Karimpour M.H., C.R. Stern, G Lang Farmer, M. Moradi, *"Geology and petrology of two distinct*

types of granitoids, Eastern Najmabad, Ghonabad, Iran.",Geological Society of America (GSA) 2009.

[22] Taylor S.R., McLennan S.M., *"The geochemical evolution of the continental crust"*, Rev. Geophys., 33, (1995) 241-265.

[23] Boynton W.V., *"Cosmochemistry of the rare earth elements: Meteorite studies"*, In: Rare earth element geochemistry. Henderson, P. (ed.), Elsevier Sci. Publ. Co., Amsterdam, (1984) 63–114.

[24] Ishihara S., *"The magnetite-series and ilmenite-series granitic rocks"*, Mining Geology 27, (1977) 293–305.

[25] Loewy S.L., Connelly J.N., Dalziel I.W.D., *"An orphaned basement block: The Arequipa-Antofalla basement of the central Andean margin of South America"*, GSA Bulletin, v. 116, (2004) 171-187.

[26] Bennett V.C., DePaolo D.J., *"Proterozoic crustal history of the western United States as determined by Nd isotope mapping",* Geol. Soc. Am. Bull. v. 99, (1987) 674-685.

[27] DePaolo D.J., *"Neodymium isotopes in the Colorado Front Range and crust-mantle evolution in the Proterozoic",* Nature, v. 291 (1981) 193-196.

[27] DePaolo D.J., *"Neodymium isotopes in the Colorado Front Range and crust-mantle evolution in the Proterozoic",* Nature, v. 291 (1981) 193-196.

[28] Thompson A. B., *"Dehydration melting of pelitic rocks and the generation of H_2O-undersaturated granitic liquids"*, American Journal of Science 282, (1982) 1567-1595.

[29] Vielzeuf D., Holloway J.R., *"Experimental determination of the liquid-absent melting relations in the pelitic system. Consequences for crustal differentiation"*, Contribution to Mineralogy and petrology 98, (1988) 257-76.

[30] Peterson J.W., Newton R.C., *"Reversed experiments on biotite-quartz-feldspar melting in the system KMASH: implications for crustal anatexis"*, Journal of Geology 97,(1989) 465-486.

[31] Holtz F., Johannes W., *"Genesis of peraluminous granites I. Experimental investigation of melt compositions at 3 and 5 kbar and various H2O activities"*, Journal of Petrology 32, (1991) 935-58.

[32] Patin˜o-Douce A.E., Johnston D.A., *"Phase equilibria and melt productivity in the pelitic system: implication for the origin of peraluminous granitoids and aluminous granulites"*, Contribution to Mineralogy and Petrology 107, (1991) 202-18.

[33] Gardien V., Thompson A. B., Grujic D., Ulmer P., *"Experimental melting biotite + quartz Muscovite assemblages and implications for crustal melting"*, Journal of Geophysical Research 100, B8, (1995) 15581-15591.

[34] Patin˜o-Douce A.E., Harris N., *"Experimental constraints on Himalayan anatexis"*, Journal of Petrology 39, (1998) 689– 710.

[35] Annen C., Bluny J.D., Sparks R.S.J., *"The Genesis of Intermediate and Silicic Magmas in Deep Crustal Hot Zones"*, Journal of Petrology 47(3), (2006) 505-539.

[36] Jagoutz O., Müntener O., Ulmer P., Pettke T., Burg J.P., Dawood H., Hussain S., *"Petrology and Mineral Chemistry of Lower Crustal Intrusions: the Chilas Complex, Kohistan (NW Pakistan)",* Journal of Petrology 48, (2007) 1895-1953.

[37] Conrad W.K., Nicholls I.A., Wall V.J., *"Water-saturated and undersaturated melting of meta-aluminous and per-aluminous crustal compositions at 10 kb: evidence for the origin of silicic magmas in the Taupo volcanic zone, New Zealand, and other occurrences"*, Journal of Petrology 29, (1988) 765-803.

[38] Beard J.S., Abitz R.J., Lofgren G.H., *"Experimental melting of crustal xenoliths from kilbourne Hole, New Mexico and implication for the contamination and genesis of magmas",* Contribution to Mineralogy and petrology 115,(1993) 88-103.

[39] Beard J.S., Lofgren G.E., *"Dehydration melting and water-saturated melting of basaltic andesitic greenstones and amphibolites at 1, 3, and 6.5 kb"*, Journal of Petrology 32, (1991)365-401.

[40] Patin˜o-Douce A.E., Beard J.S., *"Dehydration-melting of biotite gneiss and quartz*

amphibolites from 3 to 15 kbar", Journal of Petrology 36, (1995) 707-738.

[41] Springer W., Seck H.A., *"Partial fusion of basic granulites at 5 to 15 kbar: implication for the origin of TTG magmas"*, Contribution to Mineralogy and Petrology 127, (1997) 30-45.

[42] Hassanzadeh J., Daniel F. Stockli, Brian K. Horton, Gary J. Axen, Lisa D. Stockli, Marty Grove, Axel K. Schmitt, J. Douglas Walker, *"U-Pb zircon geochronology of late Neoproterozoic–Early Cambrian granitoids in Iran: Implications for paleogeography, magmatism, and exhumation history of Iranian basement"*, Tectonophysics 451 (2008) 71–96.

[43] Veevers J.J., *"Pan-African is Pan-Gondwanaland: oblique convergence drives rotation during 650–500 Ma assembly"*, Geology 31,(2003) 501–504.

[44] Ramezani Jahandar, Robert D. Tucker, *"The Saghand region, centeral Iran: U-Pb geochronology, petrogenesis and implications for Gondwana tectonics American Journal of Science"*, Vol. 303, September,(2003) 622–665.